

Article

Oxygen Isotopes from Apatite of Middle and Late Ordovician Conodonts in Peri-Baltica (The Holy Cross Mountains, Poland) and Their Climatic Implications

Wiesław Trela ^{1,*} , Ewa Krzemińska ², Karol Jewuła ³  and Zbigniew Czupyt ² 

¹ Polish Geological Institute—National Research Institute, Holy Cross Mountains Branch in Kielce, Zgoda 21, 25-953 Kielce, Poland

² Polish Geological Institute—National Research Institute, Rakowiecka 4, 00-975 Warszawa, Poland; ewa.krzeminska@pgi.gov.pl (E.K.); zbigniew.czupyt@pgi.gov.pl (Z.C.)

³ Institute of Geological Science, Polish Academy of Sciences, Senacka 1, 31-002 Kraków, Poland; k.jewula@ingpan.krakow.pl

* Correspondence: wieslaw.trela@pgi.gov.pl

Abstract: This report provides oxygen isotopes from apatite of late Middle and Late Ordovician conodonts from the southern Holy Cross Mountains in south-eastern Poland. It was a unique time interval characterised by a significant change in the Ordovician climate, tectonic, and ocean chemistry. In the Middle and early Late Ordovician, the Holy Cross Mountains were located in the mid-latitude climatic zone at the southwestern periphery of Baltica; therefore, the $\delta^{18}\text{O}_{\text{apatite}}$ values from this region provide new data on the $^{18}\text{O}/^{16}\text{O}$ budget in the Ordovician seawater reconstructed mainly from the tropical and subtropical realms. Oxygen isotopes from mixed conodont samples were measured using the SHRIMP IIe/MC ion microprobe in the Polish Geological Institute in Warsaw. The $\delta^{18}\text{O}_{\text{apatite}}$ values range from 16.75‰_{VSMOW} to 20.66‰_{VSMOW} with an average of 18.48‰_{VSMOW}. The oxygen isotopes from bioapatite of the studied section display an increasing trend, suggesting a progressive decrease in sea-surface temperature roughly consistent with an overall cooling of the Ordovician climate. Two distinctive positive excursions of $\delta^{18}\text{O}_{\text{apatite}}$ have been reported in the upper Sandbian and middle Katian of the studied section and correlated with cooling events recognised in Baltica. They are interpreted as an isotope temperature proxy of climate changes triggered by a growing continental polar ice cap, but increased $\delta^{18}\text{O}_{\text{apatite}}$ in the late Sandbian contradicts recently postulated climate warming during that time in subtropical Laurentia.

Keywords: oxygen isotopes; conodonts; Ordovician; palaeotemperature; climate



Citation: Trela, W.; Krzemińska, E.; Jewuła, K.; Czupyt, Z. Oxygen Isotopes from Apatite of Middle and Late Ordovician Conodonts in Peri-Baltica (The Holy Cross Mountains, Poland) and Their Climatic Implications. *Geosciences* **2022**, *12*, 165. <https://doi.org/10.3390/geosciences12040165>

Academic Editors: Jesus Martinez-Frias and Genming Luo

Received: 22 November 2021

Accepted: 28 March 2022

Published: 7 April 2022

Publisher's Note: MDPI stays neutral with regard to jurisdictional claims in published maps and institutional affiliations.



Copyright: © 2022 by the authors. Licensee MDPI, Basel, Switzerland. This article is an open access article distributed under the terms and conditions of the Creative Commons Attribution (CC BY) license (<https://creativecommons.org/licenses/by/4.0/>).

1. Introduction

The Ordovician period was characterised by a progressive climate change from the warm (greenhouse) to cold (icehouse) conditions that culminated in a short glacial interval confined to the Hirnantian [1–7]. The precise time of this climate transition is a matter of debate in which there are arguments for the formation of the continental polar ice cap in the early Katian or late Sandbian [8,9], or even in the late Middle Ordovician [10]. It should be noted that the transition from the Middle to Late Ordovician is characterised by a major shift in seawater $^{87}\text{Sr}/^{86}\text{Sr}$ and $\delta^{18}\text{O}$, which is linked with climate and tectonic changes [11,12]. The scenario of pre-Hirnantian climate cooling and the southern polar ice sheet formation is supported by positive $\delta^{13}\text{C}$ excursion in the lower Katian (referred to as the Guttenberg Carbon Isotope Excursion—GICE) that corresponds to eustatic sea-level fall (see [13,14] and references therein). A postulated driver of the Late Ordovician climate cooling includes decreasing $p\text{CO}_2$ level ([4,7] and references therein), although the contribution of volcanic activity is also considered via weathering of fresh volcanic glasses and high emission of SO_2 that increased the planetary albedo [9,15].

A general trend in Ordovician climate change was recognised by measurements of $\delta^{18}\text{O}$ from conodont apatite and brachiopod calcite [5,9,11,16–22]. Conodont bioapatite is relatively resistant to diagenetic alteration of $\delta^{18}\text{O}$ and thus facilitates the preservation of the original temperature signal, and it is widely used to estimate palaeotemperature (see [5,23–26]). The $\delta^{18}\text{O}_{\text{apatite}}$ data from conodonts provided by Trotter et al. [5] reveal a steady cooling trend in the Ordovician climate, including (1) progressive decrease in sea-surface temperature from the Tremadocian to early Darriwilian; (2) climate stabilisation in the middle Darriwilian to middle Katian time with seawater temperatures similar to present-day equatorial regions; and (3) a major cooling since the late Katian. This gradual climate cooling is considered to be a key factor driving major marine biodiversity culminating in the Middle Ordovician, referred to as the Great Ordovician Biodiversification Event—GOBE [5,27]. Numerous papers have concentrated on analyses of $\delta^{18}\text{O}_{\text{apatite}}$ from the late Sandbian–Katian time as this period is considered as a transitional interval from the greenhouse to icehouse conditions in the Ordovician climate [9,17–19,28,29].

This paper presents new $\delta^{18}\text{O}_{\text{apatite}}$ measurements from the Ordovician conodonts from the southern Holy Cross Mountains in SE Poland (Figure 1A; Table 1). Our results provide $\delta^{18}\text{O}_{\text{apatite}}$ data from, to date, a poorly recognised mid-latitude climatic zone of the late Middle and Late Ordovician (see new data of Albanesi et al. [20] and Männik et al. [21]). Until now, $\delta^{18}\text{O}_{\text{apatite}}$ values from Ordovician conodonts have been broadly analysed on samples from the tropical and subtropical realms; therefore, data from mid-latitudes are an important supplement to the oxygen isotope dataset for the reconstruction of the $^{18}\text{O}/^{16}\text{O}$ budget in the Ordovician oceans.

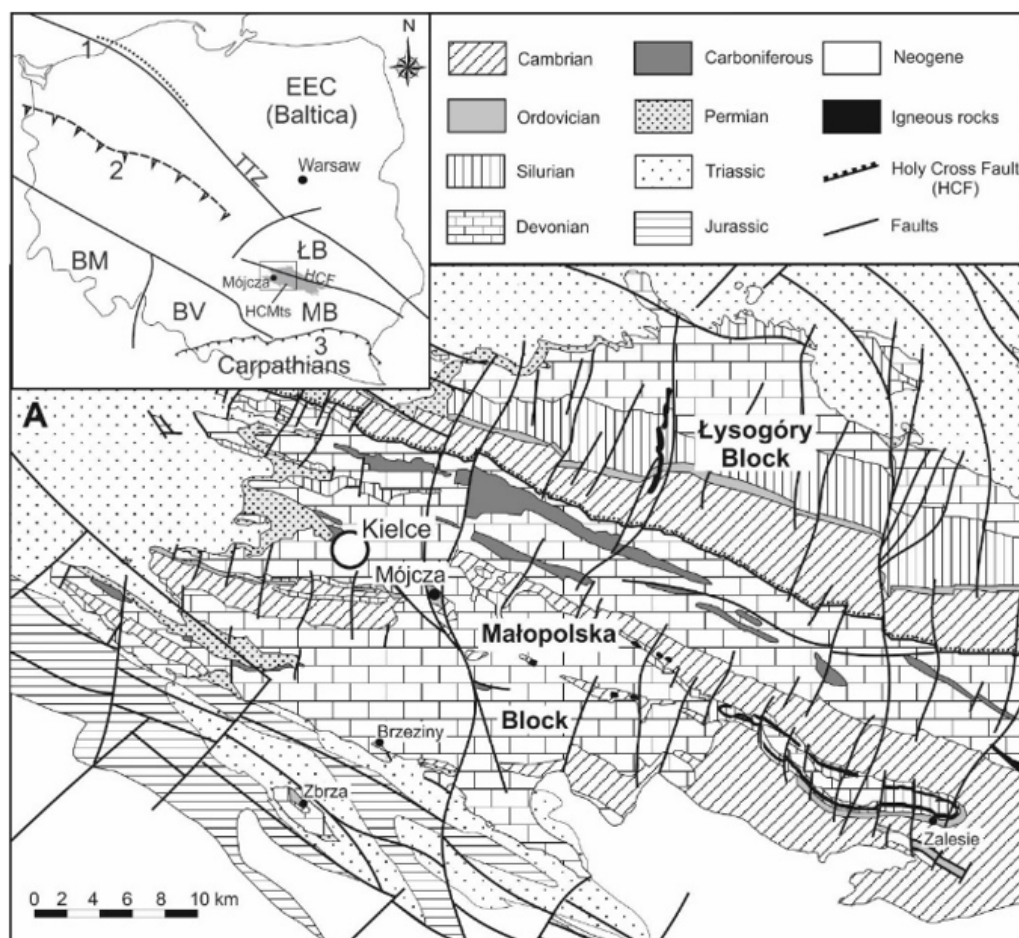


Figure 1. Cont.

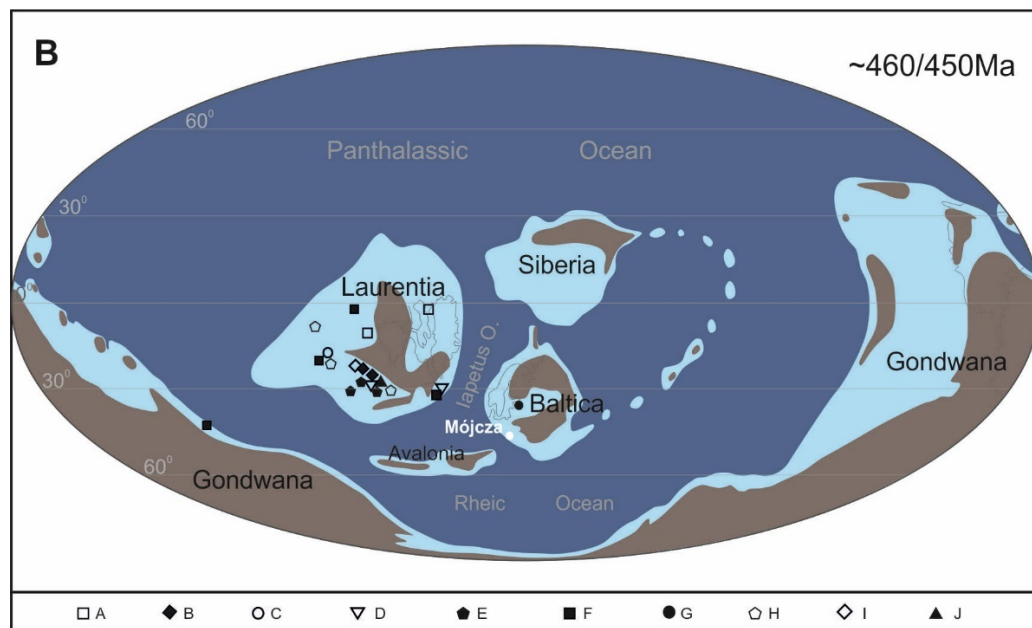


Figure 1. (A) Geological map of the western Holy Cross Mountains (without Pleistocene deposits, after Czarnocki [30] and Dadlez et al. [31], modified) and locality of the Mójcza section, EEC—East-European Craton, LB—Łysogóry Block, MB—Małopolska Block, BV—Brunovistulia block, BM—Bohemian Massive, TTZ—Teisseyre-Tornquist Tectonic Zone, HCF—Holy Cross Fault, 1—Caledonian front, 2—Variscan front, 3—Alpine front. (B) Palaeogeographic locality of the Mójcza section in the late Middle-Late Ordovician (palaeogeography from Scotese [32], modified) and other localities documenting $\delta^{18}\text{O}_{\text{apatite}}$ in the same stratigraphic interval (A—Trotter et al. [5]; B—Buggisch et al. [9]; C—Rosenau et al. [17]; D—Elrick et al. [18]; E—Quinton et al. [19]; F—Albanesi et al. [20]; G—Männik et al. [21]; H—Edwards et al. [22]; I—Herrmann et al. [28]; J—Quinton and MacLeod [29]).

Table 1. Oxygen isotopic results from the Middle and Late Ordovician conodonts of the Mójcza section.

Sample	Stages	Conodonts	No. Conodonts per Sample	No. Analyses	$\delta^{18}\text{O}$ mean [‰VSMOW]	Std. Error \pm	Std. Dev.
M1	Darriwilian	B, NI	8	35	16.99	0.16	0.95
M2		B, P, NI	8	35	16.75	0.13	0.75
M3		B, P, NI	7	28	17.29	0.18	0.96
M4		B, D, NI	7	23	17.06	0.14	0.68
M5		B, P, NI	7	27	17.68	0.16	0.85
M6		A, D, NI	6	14	17.11	0.23	1.08
M7		B, P, NI	4	11	17.82	0.30	0.99
M8	Sandbian	B, P, NI	8	32	17.80	0.20	1.09
M9		A, NI	4	14	19.00	0.19	0.71
M10		A, NI	6	22	19.59	0.20	0.95

Table 1. Cont.

Sample	Stages	Conodonts	No. Conodonts per Sample	No. Analyses	$\delta^{18}\text{O}$ mean [‰VSMOW]	Std. Error \pm	Std. Dev.
M11		B, NI	6	20	19.10	0.37	1.66
M12		A, B, NI	5	10	18.36	0.53	1.73
M13		A, B, NI	5	14	18.42	0.31	1.17
M14		A, S, NI	4	12	19.63	0.30	1.03
M15		A, S, NI	7	24	19.46	0.12	0.59
M16	Katian	S, A, H, NI	6	22	19.40	0.09	0.43
M17		A, S, NI	4	14	20.66	0.24	0.89
M18		A, H, NI	4	15	18.68	0.28	1.12
M19		A, S, NI	4	12	18.70	0.19	0.65
M20		A, NI	5	22	19.36	0.21	0.98
M21		A, NI	7	25	18.12	0.22	1.11

B—Baltoniodus sp., D—Drepanoistodus sp., P—Panderodus sp., A—Amorphognathus sp., S—Scabbardella sp., H—Hamarodus sp., NI—not identified.

2. Geological and Palaeogeographic Outline

The Holy Cross Mountains (HCMts) represent a hilly area with the Palaeozoic inlier traditionally divided into the Łysogóry Region in the north and the Kielce Region in the south (Figure 1A). They are parts of two large tectonic units exposed in this area: the Łysogóry Block in the north and Małopolska Block in the south, separated by the Holy Cross Fault (Figure 1A). The cratonic crust of the Łysogóry Block is similar to the East European Craton located north-eastward, and this tectonic unit is considered as a proximal terrane of Baltica ([33] and references therein). This is consistent with palaeomagnetic data [34] and Nd isotope data from the Upper Cambrian deposits [35]. In turn, the Małopolska Block is considered either as a proximal terrane of Baltica accreted to this palaeocontinent in the late Silurian–earliest Devonian [34,36] or an exotic terrane of the peri-Gondwanan origin attached to Baltica in the early late Cambrian (see [35,37]) or in the earliest Devonian ([33], and references therein). The palaeomagnetic data indicate that in the Middle Ordovician, the Małopolska Block was located close to its present-day position in relation to Baltica [34,38], in the mid-latitude zone of the southern hemisphere (Figure 1B) and moved close to 30° S in the Hirnantian time [39]. Based on conodont fauna, Dzik [40] argues that a relatively wide Tornquist Sea separated the HCMs and Baltica in the Middle Ordovician.

The present-day distribution of the upper Middle and Upper Ordovician sedimentary facies in the HCMts reveals the predominance of carbonates (Figure 2) in a narrow zone extending along the northern margin of the Kielce Region (i.e., in the northern periphery of the Małopolska Block). In the Łysogóry Region and southwestern Kielce Region (Zbrza-Brzeziny), the stratigraphic equivalents of the Mójcza Formation are represented by mudrock-dominated successions (Jeleniów and Wólka formations) of the deep-water shelf (Figure 2; [41–43] and references therein).

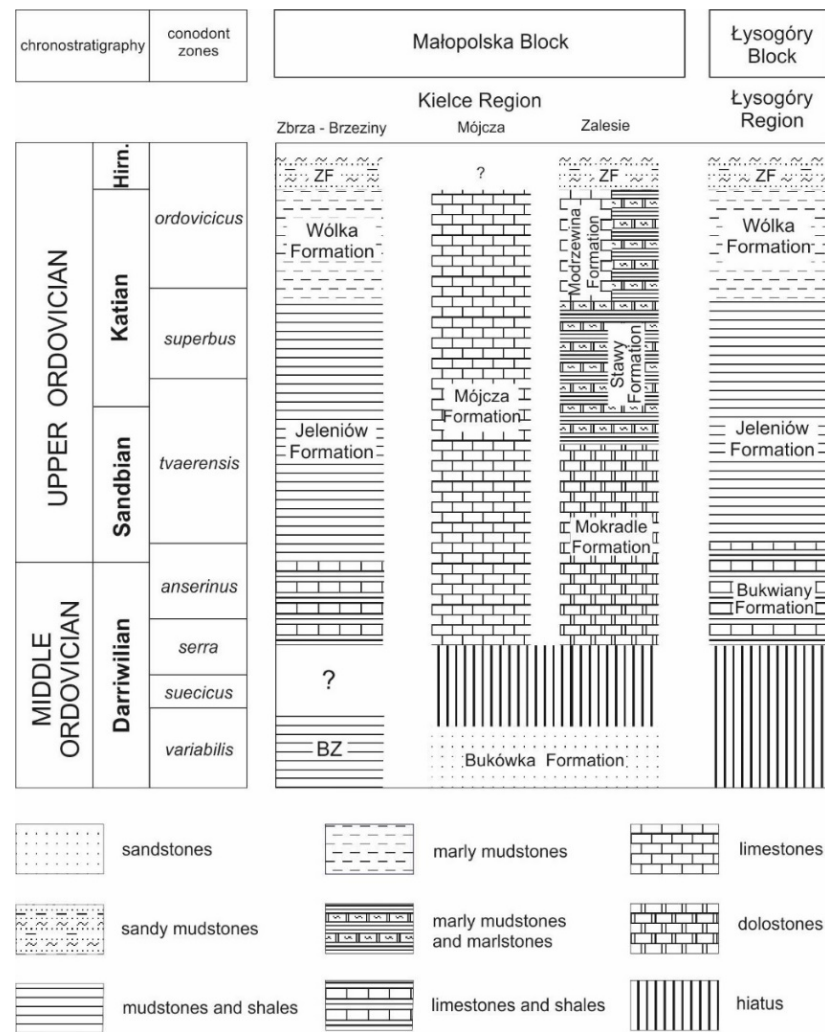


Figure 2. Lithostratigraphy of the upper Middle and Upper Ordovician, and general facies layout in the HCMts (compiled from Trela [41–43]; conodont zones after Dzik [44,45]. Hirn—Hirniantian, BZ—Brzeziny Formation, ZF—Zalesie Formation.

3. Study Section

The studied section is located in the Mójcza village south-eastward of Kielce, in the north-western Kielce Region (the northern margin of the Małopolska Block) (Figures 1 and 2). It is the type-section of the Mójcza Limestone Formation (*sensu* Trela [41]), up to a 10 m thick condensed unit. Its stratigraphic range extends from the upper Darriwilian to the upper Katian (Figure 3) and is well-dated by conodonts of the upper *serra* to *ordovicicus* zones [44,45]. The basal contact of the Mójcza Formation in this locality with the underlying calcareous sandstones and sandy limestones of the Bukówka Formation is marked by a discontinuity surface documenting the Mid-Darriwilian hiatus including the lower *serra*, *suecicus* and upper *variabilis* conodont zones [44,46]. In addition to conodonts, the fossil assemblage of the Mójcza Formation consists of trilobites, brachiopods, echinoderms, ostracods, bryozoans and molluscs [46,47]. The non-skeletal particles include phosphate ooids and carbonate and phyllosilicate oncoids, forming distinctive intervals in the uppermost Sandbian-lower Katian and the middle Katian, respectively (Figure 3; [46,47]). Based on grain components and matrix/cement types, four microfacies have been recognised in the Mójcza section, that is, (1) skeletal grainstone, or grainstone to packstone; (2) skeletal grainstone with phosphate ooids; (3) skeletal packstones to wackestones; (4) skeletal packstones with oncoids (Figure 3; see [46,47]). It is noteworthy that skeletal grains in the lower part of the section, and notably above the discontinuity surface, are coated by thin phosphatic

envelopes [46,47]. The Katian limestones are intercalated by thin (1–5 cm thick) K-bentonite beds (Figure 3), and some layers in this interval reveal ferruginous impregnated surfaces. The Mójcza Formation is overlain by up to 0.8 m thick marly mudstones (Figure 3) passing upwards into the Wenlock graptolitic shales [48].

The Mójcza Formation was formed on an isolated carbonate platform developed in the mid-latitude of SW peri-Baltica [47] dominated by temperate-water fauna [46] living in marine waters with a normal salinity. Depositional conditions on this platform were stable and characterised by a low sediment accumulation rate favouring the early diagenetic phosphate and iron authigenesis [46,47]. Moreover, from the late Darriwilian to late Sandbian, the sedimentary environment was influenced by a seasonal upwelling that delivered nutrient-rich waters from the northward-located deep-water basin [47,49].

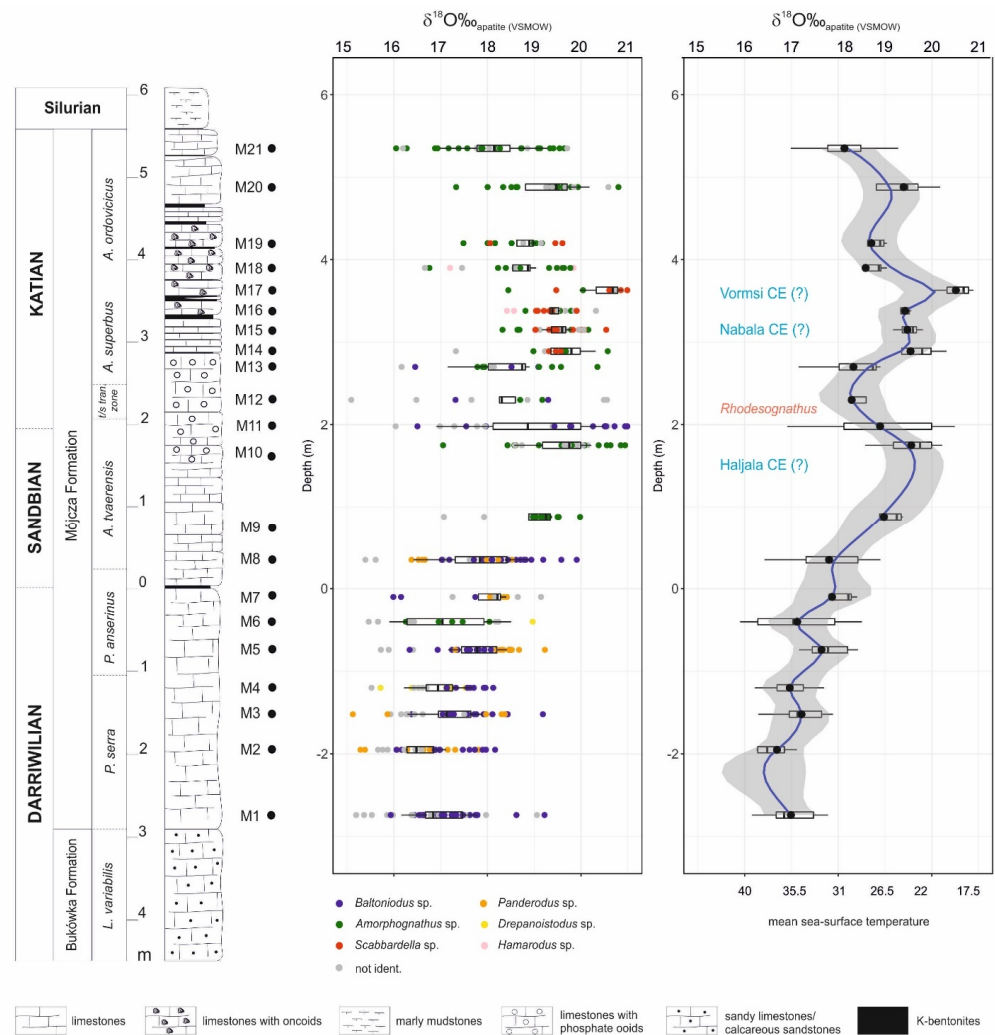


Figure 3. Oxygen isotope values from the late Middle-Late Ordovician conodonts of the Mójcza section and mean $\delta^{18}\text{O}_{\text{apatite}}$ values for each studied sample on the right (conodont zones after Dzik [44,45]). Boxplot rectangles represent data for each sample with a range between the 25th and 75th quantiles. The arithmetic mean for all measurements obtained for the sample is represented by the black dot. Whiskers indicate maximum and minimum values within the 1.5 interquartile data range. The resultant blue curve—running three-point means calculated within the R-studio Environment, using the Local Polynomial Regression Fitting (LPRF) method, with a span of 0.2. The grey interval shows a confidence interval (of 95%). The sea-surface temperature was calculated using an equation from Lécuyer et al. [50], $T [^{\circ}\text{C}] = 117.4 (\pm 0.5) - 4.5 (\pm 0.43) (\delta^{18}\text{O}_{\text{apatite}} - \delta^{18}\text{O}_{\text{seawater}})$; $\delta^{18}\text{O}_{\text{water}} = -1\text{‰}$ V-SMOW. Hirn.—Hirnantian, t/s tran. zone—*tværrensis*/*superbus* transition zone.

4. Samples and Methods

The 122 conodont elements in 21 samples from the Mójcza section were measured for the $\delta^{18}\text{O}$ value by secondary ion mass spectrometry (SIMS) using SHRIMP IIe/MC ion microprobe (Table 1; Supplementary Materials Tables S1 and S2). They cover the stratigraphic interval from the upper Darriwilian to the late Katian. Conodont elements were extracted from crushed limestone samples fully dissolved in a 10% acetic acid. The residual material was sieved, and then conodonts were selected using a steel needle. Oxygen isotope analyses were performed on ramiform and coniform conodont elements (usually fragmented) without preserved basal filling. Samples consisted of mixed specimens that included unidentified elements and different taxa such as *Baltoniodus*, *Panderodus*, *Drepanoistodus*, *Amorphognathus*, *Scabbardella* and *Hamarodus* (Supplementary Materials Table S1) extracted from 10–15 cm thick beds. They reveal a low Colour Alteration Index (CAI) of no more than 1 [51,52].

Oxygen isotopes from conodont apatite were measured using the SHRIMP IIe/MC ion microprobe in the Polish Geological Institute-National Research Institute in Warsaw, according to the general analytical procedure of bioapatite in situ measurements developed in the SHRIMP laboratory of the Research School of Earth Sciences at Australian National University [5,53,54]. Selected conodont specimens and the primary Durango apatite standard were placed on a double-stick tape with sufficient orientation inside a circle of 35 mm in diameter, forming a megamount. The conodonts were arranged in rows, but Durango apatite chips (internal standard) were placed in the centre. Prepared samples were flooded by EpoFix Stuers resin. After hardening, the megamounts were cut and ground to a thickness of ~5 mm and polished to expose cross-sections of conodont and apatite standards, and washed with ethanol and ultrasonically cleaned with deionised water. Reflected (RL) and transmitted light (TL) imaging was conducted before the analytical session. This documentation was the basis for the preselection of the spot location. The Au-coated mounts were stored in the instrument chamber for SIMS analyses. In situ measuring procedures in this study are similar to those previously reported by Narkiewicz et al. [55] and Rigo et al. [54]. Two to seven measurements were made in each conodont element on the uniform surface devoid of apparent heterogeneities. The Cs^+ primary ion beam was accelerated at 15 kV, with an intensity of ca. 3.5 nA. Oxygen isotopes were measured using the “multi-collection” mode.

The mass resolution used to measure oxygen isotopes was ca. 1800, counted at 10% of the height of the peak. The measurement of oxygen isotopes included two sets for six scans of ^{16}O - and ^{18}O mass measured simultaneously on Faraday’s cups. The total measurement time of one point was about 7 min, including 120 s seconds of rastering. All the SHRIMP analyses were referred to the primary apatite standard Durango 3 (see Supplementary Materials Table S2) according to that described by Trotter et al. [53] with a $\delta^{18}\text{O}$ composition of $9.8 \pm 0.25\text{‰}$ determined by gas isotope ratio mass spectrometry (GIRMS) and normalised to NBS120c = 21.7‰. Isotope values are reported in the standard Vienna Standard Mean Ocean Water scale (V-SMOW).

Each analytical session (usually <200 analyses to minimise the instrumental drift) was monitored by measuring the Durango standard every 3–4 sample analyses. Statistical reduction of the collected data was performed separately for each session using POXI MC v 2.9 software, developed in-house at the Australian National University.

The standard deviation of Durango by SHRIMP analyses was 0.15–0.45‰ with a regular number ($n = 19$ –22) of standard analyses for each session.

5. Results

The measured $\delta^{18}\text{O}_{\text{mean}}$ values from conodont taxa in the Mójcza section range from 16.75 to 20.66‰_{VSMOW} with an average of 18.48‰_{VSMOW} (Table 1; Supplementary Materials Table S1). Mean standard deviations of $\delta^{18}\text{O}$ from studied conodont samples range from 0.43‰ (sample M16) to 1.73‰ (sample M12) (Table 1; Supplementary Materials Table S1). The minimum and maximum values of $\delta^{18}\text{O}_{\text{mean}}$ from conodonts of the same sample differ

from 0.8 (sample M16) to 4.18‰ (samples M10, M13) (Supplementary Materials Table S1). In ten samples, this difference is in the range of 1.0–1.8‰ (M1, M2, M3, M4, M7, M14, M17, M18, M19, M20), and only in three samples, it is less than 1‰ (M9, M15, M16), whereas in three samples this difference is ~2.5‰ (M5, M6, M8). In five samples (M10, M11, M12, M13, M21), the difference is even higher, and ranges as high as 3.4–4.18‰ (Supplementary Materials Table S1).

In the upper Darriwilian to lower Sandbian interval, the oxygen isotope analyses show a general increasing trend with slightly variable $\delta^{18}\text{O}_{\text{apatite}}$ values scattered around the baseline value ~17.5‰, ranging from 16.75‰ to 17.82‰ (Table 1; Figure 3). Their comparison with SIMS-based measurements from the other localities indicates that values from the Darriwilian–Sandbian transition (samples M5, M7, M8) are within a similar range to those reported by Albanesi et al. [20] from Precordillera and Laurentia (the Marathon area in Texas) (Figure 4). Furthermore, our data from this interval are similar to the single sample (8119; 17.8‰) from the middle Sandbian [5], and they are in the lower range of SIMS-based $\delta^{18}\text{O}_{\text{apatite}}$ values from the Antelope Range in Nevada [22] (Figure 4).

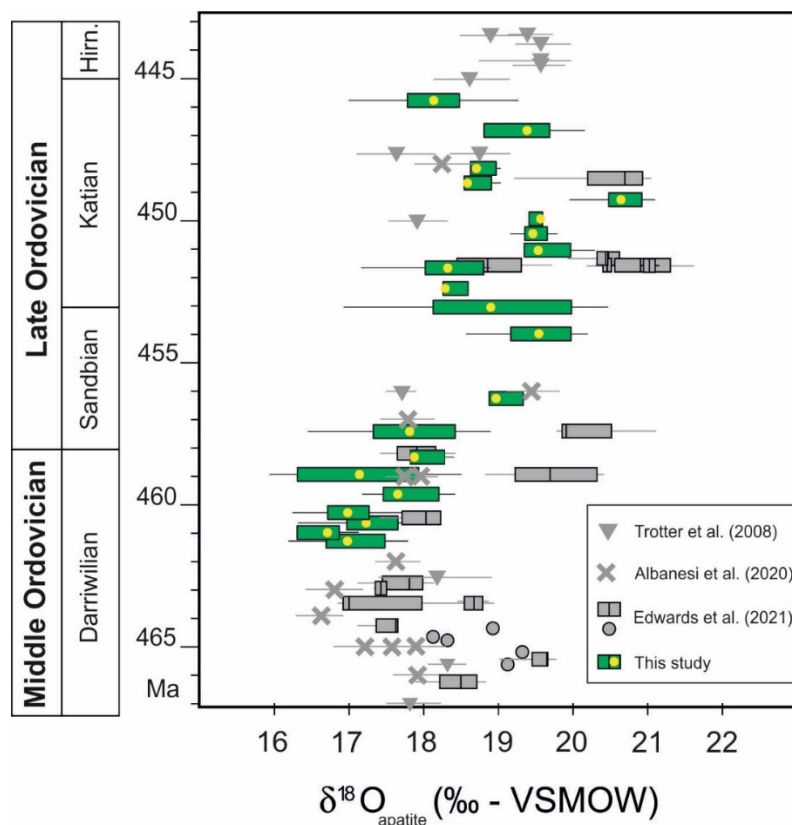


Figure 4. $\delta^{18}\text{O}_{\text{apatite}}$ values from this study and SIMS-based data from the literature Trotter et al. [5], Albanesi et al. [20], Edwards et al. [22] plotted relative to the Ordovician time scale Cooper et al. [56]. The location of studied samples on the time scale is approximately determined on the conodont zone assignment.

An increasing trend continues in the middle Sandbian–Katian interval and shows a shift of the baseline value to ~19‰ (Figure 3). The $\delta^{18}\text{O}_{\text{apatite}}$ values in this part of the Mójcza section are more variable and vary between 18.12 and 20.66‰ (Table 1; Figure 3). The two highest $\delta^{18}\text{O}_{\text{apatite}}$ values in the Mójcza section have been reported in this interval, and they reach 19.59 and 20.66‰ (samples M10 and M17), respectively (Table 1; Figure 3). The lower positive shift occurs in the upper Sandbian within the upper *toaerensis* conodont zone, whereas the second excursion correlates with the middle Katian and the boundary of the *superbus/ordovicicus* zones (Figure 3). An increasing trend in the lower excursion

starts already in the middle Sandbian, as can be inferred from the sample M9 that shows a comparable value to SIMS-based analysis from the same stratigraphic interval in Precordillera [20] (Figure 3; Figure 4). In turn, the $\delta^{18}\text{O}_{\text{apatite}}$ values from the lower-middle Katian transition are generally within the same range as measurements from the Cincinnati Arch region of Kentucky and Indiana (Laurentia) but, compared to our data, most values from the USA are above 20‰ [22]. The $\delta^{18}\text{O}_{\text{apatite}}$ analyses from the upper Katian of the HCMts are nearly the same as SIMS-based measurements from Laurentia provided by Trotter et al. [5] and Albanesi et al. [20] (Figure 4).

Numerous $\delta^{18}\text{O}_{\text{apatite}}$ values from the late Sandbian–Katian conodonts have been provided from Laurentia [9,17–19,22,28] and Baltica [21] measured using a high-temperature conversion-elemental analyser (TC-EA) coupled online to a mass spectrometer. However, the comparison of $\delta^{18}\text{O}_{\text{apatite}}$ values obtained from the TC-EA method with the SIMS-based data needs correction since the latter is usually higher, and an empirically estimated offset between these methodologies is $\sim 1.0\text{‰}$ (see [22,53,57]). With this correction (average -1‰), our data from the upper Sandbian–Katian are generally in the same range as those from the cited above papers, but most of them are scattered around an average of 18.5‰.

6. Discussion

It is assumed that conodont $\delta^{18}\text{O}$ is dependent on the oxygen isotope composition, temperature, and salinity of the ambient seawater. However, evidence shows that individual conodont species can reveal an offset of $\delta^{18}\text{O}_{\text{apatite}}$ values related to their different palaeoecology and life habits [16,28,29,58,59]. In addition, Wheeley et al. [58] have reviewed the effects of the thermal alteration and sample processing and extraction methods on the oxygen isotope signature of conodont samples. The application of analytical protocols proposed by these authors may contribute to obtaining more reliable $\delta^{18}\text{O}$ values. Despite post-mortem artefacts, the oxygen isotope studies of conodonts are considered reliable tools for tracing seawater palaeotemperature evolution and climate changes [5,24,25,60,61].

6.1. Calculation of Palaeotemperatures

The fossil fauna of the carbonate Mójca platform indicates normal marine salinity of ambient seawater [46,47]. The low CAI of studied conodonts allows the assumption that they were not deeply buried and devoid of a significant thermal alteration, affecting oxygen isotope values.

Calculation of sea-surface palaeotemperature from bioapatite is based on the widely accepted assumption that, in non-glacial periods of Phanerozoic, the $\delta^{18}\text{O}$ for normal seawater was -1‰ [5,16,53,61]. However, it should be noted that the $^{18}\text{O}/^{16}\text{O}$ budget of ocean waters over the geologic time is still under discussion, and an opposite concept implies increasing seawater $\delta^{18}\text{O}$ through Phanerozoic with superimposed short-term oscillations corresponding to glacial episodes ([62–66] and references therein).

Palaeotemperatures from $\delta^{18}\text{O}_{\text{apatite}}$ of studied conodonts were calculated using the equation of Lécuyer et al. [50]: $T(^{\circ}\text{C}) = 117.4 (\pm 9.5) - 4.5 (\pm 0.43) (\delta^{18}\text{O}_{\text{apatite}} - \delta^{18}\text{O}_{\text{seawater}})$ but the estimated temperature may differ depending on the palaeotemperature equation used, and may even be up to 8 °C [67–69]. Moreover, some authors highlight that the correct $\delta^{18}\text{O}$ value for NBS-120c is uncertain and, therefore, may be responsible for a further variation of $\sim 4\text{ °C}$ (see [67,70]).

Considering the low CAI of studied conodonts and normal marine salinity, and the ice-free pre-Hirnantian seawater $\delta^{18}\text{O}$ value of -1.0‰ V-SMOW, the calculated mean sea-surface temperatures from SIMS-based $\delta^{18}\text{O}_{\text{apatite}}$ (16.75 to 20.66‰) are within the wide range between 38 and 20 °C. The $\delta^{18}\text{O}_{\text{apatite}}$ values from the upper Darriwilian conodonts indicate that the mean sea-surface temperature in that time varied between 35 and 38 °C, and then dropped to 33 °C ($\delta^{18}\text{O}_{\text{apatite}} = 17.82\text{‰}$) in the transition to the lower Sandbian (samples M7 and M8; Figure 3, Table 1). This palaeotemperature range is clearly higher than predicted sea-surface temperatures for mid-latitudes in the late Middle-Late Ordovician time (see [4,71]). Moreover, it must be noted that 38 °C is the upper temperature limit that is

lethal for modern marine animals, and this limit can also be applied to the Ordovician fauna. The calculated palaeotemperatures for the late Sandbian and middle Katian $\delta^{18}\text{O}_{\text{apatite}}$ positive excursions would indicate a decrease to 25 °C (sample M10) and 20 °C (sample M17), respectively (Figure 3).

6.2. Variability of $\delta^{18}\text{O}_{\text{apatite}}$ in a Climatic Context

Conodont samples from the Mójca Formation display an increase in mean $\delta^{18}\text{O}_{\text{apatite}}$ values since the late Darriwilian to late Katian, which can be interpreted in the palaeoclimatic context as gradual cooling during this time. However, this general assumption contradicts the stabilisation of the Ordovician climate from the middle Darriwilian to middle Katian with sea-surface temperatures similar to the present-day equatorial regions [5]. It should be noted that the sampling resolution through this interval in Trotter et al. [5] is too low to discern any climatic changes in this time interval. Our data suggest a more variable oxygen isotope record through the upper Darriwilian to middle Katian roughly consistent with the increasing $\delta^{18}\text{O}_{\text{apatite}}$ trend documented in the coeval stratigraphic interval from Estonia [21] and China [72]. The Estonian $\delta^{18}\text{O}_{\text{apatite}}$ data are particularly important for a comparative analysis with our results since in the Ordovician both areas were palaeogeographically related to Baltica. In addition, the high-resolution Estonian data provide insights into oxygen isotope changes characterised by distinct cooling events in the Late Ordovician epicontinental sea [21].

The conodont specimens predominating in the studied samples are represented by taxa with a pelagic mode of life that preferred a shallow-water (e.g., *Baltoniodus*, *Panderodus*) to relatively deeper-water (e.g., *Scabbardella*, *Amorphognathus*) environment (see [44,73,74]). However, it is noteworthy that Sweet [73] suggests that at low-latitude sites, *Amorphognathus* occupied the deeper-water setting in contrast to high latitudes, and points out that the distribution of this species was mainly controlled by temperature, not depth. The identification of studied conodonts at the genus level and the presence of unidentified specimens make detailed palaeoecological interpretation of the obtained oxygen isotope analyses difficult; therefore, we focused on an overall isotopic trend and its climatic implication. Increasing $\delta^{18}\text{O}_{\text{apatite}}$ values in the Mójca section suggest a gradual decrease in sea-surface temperature from the late Darriwilian (also postulated by Rasmussen et al. [10]) with the first climax (19.59‰ in sample M10) in the late Sandbian (Figure 3). The three-point running $\delta^{18}\text{O}_{\text{apatite}}$ curve evidently indicates a significant increasing trend through the Sandbian (Figure 3); however, a low sampling resolution in this interval precludes a more precise climatic interpretation. Notably, the first significant shift of $\delta^{18}\text{O}_{\text{apatite}}$ is within the upper *tværensis* conodont zone and appears to correspond to the Estonian Haljala cooling event (see [21]). This isotopic shift correlates with intense bioturbation and benthic oxygenation in the deep-water shelf of the northern HCMts and coincides with the late Sandbian sea-level fall preceding the expansion of anoxic conditions during the early Katian transgression [43,75]. Furthermore, the discussed $\delta^{18}\text{O}_{\text{apatite}}$ shift occurs in the time characterised by intensified volcanic activity evidenced by numerous ash beds in Laurentia and Baltica (see [76–80]). An increase in $\delta^{18}\text{O}_{\text{apatite}}$ values in the late Sandbian has also been noted in Laurentia [9,28], at the Sandbian/Katian boundary in China [72], and in the middle Sandbian from Precordillera [20]. The positive $\delta^{18}\text{O}_{\text{apatite}}$ excursion in Laurentia has been linked by Buggisch et al. [9] with climate cooling driven by intense volcanism evidenced by the Deicke ash bed. This hypothesis has been challenged by Herrmann et al. [28], who estimated fluctuations of ocean temperatures at that time based on oxygen isotopes from conodonts and did not find climatic perturbations associated with the volcanic eruption; instead, they suggested the pre-Deicke cooling.

A ~1.2‰ drop of the $\delta^{18}\text{O}_{\text{apatite}}$ values in samples M12 and M13 compared to M10 can correspond to the early Katian warming recorded in Laurentia [19,28,29]. In this part of the Mójca section, Dzik [44,45,81] noted the occurrence of warm-water *Rhodesognathus* in the conodont assemblage. The following highest $\delta^{18}\text{O}_{\text{apatite}}$ excursion in the Mójca section occurring in the middle Katian (sample M 17, Figure 3) appears to be coeval to the

Estonian early Nabala or Vormsi cooling events extending across the *superbus/ordovicicus* conodont zones (see Männik et al. [21]). An increase in $\delta^{18}\text{O}_{\text{apatite}}$ to 20.66‰ suggests a temperature drop by 4–5 °C compared to samples M15 and M16. It is noteworthy that the main excursion in the lower *ordovicicus* zone (sample M17) was preceded by a slight increase in the $\delta^{18}\text{O}_{\text{apatite}}$ to 19.63‰ (sample M14) in the upper *superbus* zone (Figure 3; Table 1). Such a value was originally recorded by Trotter et al. [5] in the Hirnantian conodonts from the subtropical zone of Laurentia. So, this two-stage middle Katian excursion in the condensed Mójcza section may be an isotope signature of two short-term climate shifts corresponding to the Nabala and Vormsi cooling events, respectively. Moreover, this Katian shift is coeval with the increasing frequency of cool-water conodont *Scabardella*, which remained a dominating species up to the top of the Mójcza section [44,81]. The middle Katian $\delta^{18}\text{O}_{\text{apatite}}$ positive shift correlates with increased benthic oxygenation in the northern HCMts [43] produced by a significant change in ocean circulation due to polar cooling [75].

It should be noted that, as discussed above, cooling events in the late Sandbian to middle Katian of the HCMts seem at odds with stable and warm climate conditions recorded during this time in Laurentia [19,28,29]. On the other hand, Elrick et al. [18] provided $\delta^{18}\text{O}_{\text{apatite}}$ data for orbital-scale glacioeustasy and related changes in ice volume and sea-surface temperatures in the Katian time. Furthermore, fluctuations of the $\delta^{18}\text{O}_{\text{apatite}}$ across the Sandbian–Katian transition in southern Oklahoma are interpreted as climatic perturbations with the cooling event recorded by the positive oxygen isotope shift within the lower GICE preceded by warm climate conditions [17]. Given highly variable $\delta^{18}\text{O}_{\text{apatite}}$ values recorded in the Haljala Regional Stage in Estonia [21] and data from the HCMts, we can infer that the climate in the late Sandbian of the mid-latitude belt was characterised by unstable conditions. This variability in climatic conditions persisted throughout the entire Katian. This can be supported by cold episodes documented by Dzik [45,81] in the conodont assemblage of the Mójcza section recording the migration of Gondwanan taxa to the mid-latitude zone. It seems consistent with glacioeustatic events recognised in the Katian of southern Morocco (Gondwana) based on high-resolution facies analysis [82].

7. Conclusions

The $\delta^{18}\text{O}_{\text{apatite}}$ values in the studied section reveal an increasing trend ranging from 16.75 to 20.66‰_{VSMOW}, consistent with an overall trend documented in the oxygen isotope record of other places. The three-point running $\delta^{18}\text{O}_{\text{apatite}}$ curve indicates two substantial positive excursions occurring in the upper Sandbian and middle Katian, respectively, which seem at odds with stable and warm climate conditions postulated during that time in Laurentia. However, it should be noted that positive shifts in the same stratigraphic interval have been reported in some localities of the sub-tropical and mid-latitude belts. They have been considered as the isotopic record of climate cooling and related decrease in sea-surface temperature driven by increasing ice volume. The calculated sea-surface palaeotemperature from the $\delta^{18}\text{O}_{\text{apatite}}$ shows a decreasing trend ranging from 38 °C in the late Darriwilian to 25 and 20 °C in the late Sandbian and middle Katian cooling events, respectively. However, the sea-surface palaeotemperature estimated for the late Darriwilian and early Sandbian is higher (with a temperature of 38 °C lethal for marine fauna) than predicted for mid-latitudes in that time. Our studies, together with other data from the literature, indicate a variable oxygen isotope record in the Sandbian–middle Katian interval, suggesting a more complex climate trend, at least in the mid-latitude zone; however, regional and/or seasonal controls on the $\delta^{18}\text{O}_{\text{apatite}}$ changes should also be considered.

Supplementary Materials: The following supporting information can be downloaded at: <https://www.mdpi.com/article/10.3390/geosciences12040165/s1>; Table S1: (Measurements of $\delta^{18}\text{O}_{\text{apatite}}$ by secondary ion mass spectrometry (SIMS) using SHRIMP IIe/MC ion microprobe) and Table S2 (Measured oxygen isotope values for the reference Durango apatite analysed in this study).

Author Contributions: Conceptualization, W.T.; methodology, W.T., E.K., Z.C.; formal analysis, K.J., E.K.; investigation, W.T., E.K.; resources, E.K., Z.C., W.T.; data curation, W.T.; writing—original draft preparation, W.T., E.K., K.J.; visualization, W.T., K.J.; supervision, W.T. All authors have read and agreed to the published version of the manuscript.

Funding: The publication fee was financed by The National Fund for Environmental Protection and Water Management as well as Polish Geological Institute-National Research Institute (project no. 62.9700.2200.00.1 and 61.2407.1501.00.0).



Institutional Review Board Statement: Not applicable.

Informed Consent Statement: Not applicable.

Data Availability Statement: Not applicable.

Acknowledgments: We are grateful to anonymous reviewers for their constructive comments.

Conflicts of Interest: The authors declare no conflict of interest.

References

- Frakes, L.A.; Francis, J.E.; Syktus, J.I. *Climate Modes of the Phanerozoic*; Cambridge University Press (CUP): Cambridge, UK, 1992.
- Brenchley, P.J.; Marshall, J.D.; Carden, G.A.F.; Robertson, D.B.R.; Long, D.G.F.; Meidla, T.; Hints, L.; Anderson, T.F. Bathymetric and isotopic evidence for a short-lived Late Ordovician glaciation in a greenhouse period. *Geology* **1994**, *22*, 295–298. [[CrossRef](#)]
- Sheehan, P.M. The Late Ordovician Mass Extinction. *Annu. Rev. Earth Planet. Sci.* **2001**, *29*, 331–364. [[CrossRef](#)]
- Herrmann, A.D.; Patzkowsky, M.E.; Pollard, D. The impact of paleogeography, pCO₂, poleward ocean heat transport and sea level change on global cooling during the Late Ordovician. *Palaeogeogr. Palaeoclim. Palaeoecol.* **2004**, *206*, 59–74. [[CrossRef](#)]
- Trotter, J.A.; Williams, I.S.; Barnes, C.R.; Lécuyer, C.; Nicoll, R.S. Did Cooling Oceans Trigger Ordovician Biodiversification? Evidence from Conodont Thermometry. *Science* **2008**, *321*, 550–554. [[CrossRef](#)]
- Finnegan, S.; Bergmann, K.; Eiler, J.M.; Jones, D.S.; Fike, D.A.; Eisenman, I.; Hughes, N.C.; Tripathi, A.K.; Fischer, W.W. The Magnitude and Duration of Late Ordovician–Early Silurian Glaciation. *Science* **2011**, *331*, 903–906. [[CrossRef](#)]
- Algeo, T.J.; Marengo, P.J.; Saltzman, M.R. Co-evolution of oceans, climate, and the biosphere during the ‘Ordovician Revolution’: A review. *Palaeogeogr. Palaeoclim. Palaeoecol.* **2016**, *458*, 1–11. [[CrossRef](#)]
- Saltzman, M.R.; Young, S.A. Long-lived glaciation in the Late Ordovician? Isotopic and sequence-stratigraphic evidence from western Laurentia. *Geology* **2005**, *33*, 109–112. [[CrossRef](#)]
- Buggisch, W.; Joachimski, M.M.; Lehnert, O.; Bergström, S.M.; Repetski, J.E.; Webers, G.F. Did intense volcanism trigger the first Late Ordovician icehouse? *Geology* **2010**, *38*, 327–330. [[CrossRef](#)]
- Rasmussen, C.M.Ø.; Ullmann, C.V.; Jakobsen, K.G.; Lindsbog, A.; Hansen, J.; Hansen, T.; Eriksson, M.E.; Dronov, A.; Frei, R.; Korte, C.; et al. Onset of main Phanerozoic marine radiation sparked by emerging Mid Ordovician icehouse. *Sci. Rep.* **2016**, *6*, 18884. [[CrossRef](#)]
- Shields, G.; Carden, G.A.; Veizer, J.; Meidla, T.; Rong, J.-Y.; Li, R.-Y. Sr, C, and O isotope geochemistry of Ordovician brachiopods: A major isotopic event around the Middle-Late Ordovician transition. *Geochim. Cosmochim. Acta* **2003**, *67*, 2005–2025. [[CrossRef](#)]
- Young, S.A.; Saltzman, M.R.; Foland, K.A.; Linder, J.S.; Kump, L.R. A major drop in seawater 87Sr/86Sr during the Middle Ordovician (Darriwilian): Links to volcanism and climate? *Geology* **2009**, *37*, 951–954. [[CrossRef](#)]
- Young, S.A.; Saltzman, M.R.; Bergström, S.M.; Leslie, S.A.; Xu, C. Paired $\delta^{13}\text{C}_{\text{carb}}$ and $\delta^{13}\text{C}_{\text{org}}$ records of Upper Ordovician (Sandbian–Katian) carbonates in North America and China: Implications for paleoceanographic change. *Palaeogeogr. Palaeoclim. Palaeoecol.* **2008**, *270*, 166–178. [[CrossRef](#)]
- Bergström, S.M.; Young, S.; Schmitz, B. Katian (Upper Ordovician) $\delta^{13}\text{C}$ chemostratigraphy and sequence stratigraphy in the United States and Baltoscandia: A regional comparison. *Palaeogeogr. Palaeoclim. Palaeoecol.* **2010**, *296*, 217–234. [[CrossRef](#)]
- Jones, D.; Martini, A.M.; Fike, D.; Kaiho, K. A volcanic trigger for the Late Ordovician mass extinction? Mercury data from south China and Laurentia. *Geology* **2017**, *45*, 631–634. [[CrossRef](#)]
- Bassett, D.; MacLeod, K.; Miller, J.F.; Ethington, R.L. Oxygen isotopic composition of biogenic phosphate and the temperature of early ordovician seawater. *Palaios* **2007**, *22*, 98–103. [[CrossRef](#)]
- Rosenau, N.A.; Herrmann, A.D.; Leslie, S. Conodont apatite $\delta^{18}\text{O}$ values from a platform margin setting, Oklahoma, USA: Implications for initiation of Late Ordovician icehouse conditions. *Palaeogeogr. Palaeoclim. Palaeoecol.* **2012**, *315–316*, 172–180. [[CrossRef](#)]
- Elrick, M.; Reardon, D.; Labor, W.; Martin, J.; DesRochers, A.; Pope, M. Orbital-scale climate change and glacioeustasy during the early Late Ordovician (pre-Hirnantian) determined from $\delta^{18}\text{O}$ values in marine apatite. *Geology* **2013**, *41*, 775–778. [[CrossRef](#)]

19. Quinton, P.C.; Law, S.; Macleod, K.G.; Herrmann, A.D.; Haynes, J.T.; Leslie, S.A. Testing the early Late Ordovician cool-water hypothesis with oxygen isotopes from conodont apatite. *Geol. Mag.* **2018**, *155*, 1727–1741. [[CrossRef](#)]
20. Albanesi, G.L.; Barnes, C.R.; Trotter, J.; Williams, I.S.; Bergström, S.M. Comparative Lower-Middle Ordovician conodont oxygen isotope palaeothermometry of the Argentine Precordillera and Laurentian margins. *Palaeogeogr. Palaeoclim. Palaeoecol.* **2020**, *549*, 109115. [[CrossRef](#)]
21. Männik, P.; Lehnert, O.; Nõlvak, J.; Joachimski, M.M. Climate changes in the pre-Hirnantian Late Ordovician based on $\delta^{18}\text{O}_{\text{phos}}$ studies from Estonia. *Palaeogeogr. Palaeoclim. Palaeoecol.* **2021**, *569*, 110347. [[CrossRef](#)]
22. Edwards, C.T.; Jones, C.M.; Quinton, P.C.; Fike, D.A. Oxygen isotope ($\delta^{18}\text{O}$) trends measured from Ordovician conodont apatite using secondary ion mass spectrometry (SIMS): Implications for paleo-thermometry studies. *GSA Bull.* **2021**, *134*, 261–274. [[CrossRef](#)]
23. Luz, B.; Kolodny, Y.; Kovach, J. Oxygen isotope variations in phosphate of biogenic apatites, III. Conodonts. *Earth Planet. Sci. Lett.* **1984**, *69*, 255–262. [[CrossRef](#)]
24. Wenzel, B.; Lecuyer, C.; Joachimski, M. Comparing oxygen isotope records of silurian calcite and phosphate— $\delta^{18}\text{O}$ compositions of brachiopods and conodonts. *Geochim. Cosmochim. Acta* **2000**, *64*, 1859–1872. [[CrossRef](#)]
25. Joachimski, M.M.; Von Bitter, P.H.; Buggisch, W. Constraints on Pennsylvanian glacioeustatic sea-level changes using oxygen isotopes of conodont apatite. *Geology* **2006**, *34*, 277–280. [[CrossRef](#)]
26. Quinton, P.C.; Speir, L.; Miller, J.; Ethington, R.; MacLeod, K. Extreme heat in the early ordovician. *Palaios* **2018**, *33*, 353–360. [[CrossRef](#)]
27. Servais, T.; Harper, D.A. The Great Ordovician Biodiversification Event (GOBE): Definition, concept and duration. *Lethaia* **2018**, *51*, 151–164. [[CrossRef](#)]
28. Herrmann, A.D.; MacLeod, K.; Leslie, S. Did a volcanic mega-eruption cause global cooling during the late ordovician? *Palaios* **2010**, *25*, 831–836. [[CrossRef](#)]
29. Quinton, P.C.; MacLeod, K. Oxygen isotopes from conodont apatite of the midcontinent, US: Implications for Late Ordovician climate evolution. *Palaeogeogr. Palaeoclim. Palaeoecol.* **2014**, *404*, 57–66. [[CrossRef](#)]
30. Czarnocki, J. *Ogólna Mapa Geologiczna Polski 1:100,000*; Arkusz 4, Kielce; Państwowy Instytut Geologiczny: Warszawa, Poland, 1938.
31. Dadlez, R.; Marek, S.; Pokorski, J. *Geological Map of Poland without Cenozoic deposits 1:1,000,000*; Polish Geological Institute: Warszawa, Poland, 2000.
32. Scotese, C.R. *Atlas of Silurian and Middle-Late Ordovician Paleogeographic Maps (Mollweide Projection), Maps 73–80, Volume 5, The Early Paleozoic, PALEOMAP Atlas for ArcGIS, PALEOMAP Project*; PALEOMAP Project: Evanston, IL, USA, 2014.
33. Narkiewicz, M.; Petecki, Z. Basement structure of the Paleozoic Platform in Poland. *Geol. Q.* **2017**, *61*, 502–520. [[CrossRef](#)]
34. Nawrocki, J.; Dunlap, J.; Pecskay, Z.; Krzemiński, L.; Żylińska, A.; Fanning, C.M.; Kozłowski, W.; Salwa, S.; Szczepanik, Z.; Trela, W. Late Neoproterozoic to Early Palaeozoic palaeogeography of the Holy Cross Mountains (Central Europe): An integrated approach. *J. Geol. Soc.* **2007**, *164*, 405–423. [[CrossRef](#)]
35. Walczak, A.; Belka, Z. Fingerprinting Gondwana versus Baltica provenance: Nd and Sr isotopes in Lower Paleozoic clastic rocks of the Małopolska and Łysogóry terranes, southern Poland. *Gondwana Res.* **2017**, *45*, 138–151. [[CrossRef](#)]
36. Dadlez, R.; Kowalczewski, Z.; Znosko, J. Niektóre kluczowe problemy przedpermskiej tektoniki Polski. *Geol. Q.* **1994**, *38*, 169–190.
37. Belka, Z.; Valverde-Vaquero, P.; Dörr, W.; Ahrendt, H.; Wemmer, K.; Franke, W.; Schäfer, J. Accretion of first Gondwana-derived terranes at the margin of Baltica. *Geol. Soc. London, Spéc. Publ.* **2002**, *201*, 19–36. [[CrossRef](#)]
38. Schatz, M.; Zwing, A.; Tait, J.; Belka, Z.; Soffel, H.; Bachtadse, V. Paleomagnetism of Ordovician carbonate rocks from Malopolska Massif, Holy Cross Mountains, SE Poland—Magnetostatigraphic and geotectonic implications. *Earth Planet. Sci. Lett.* **2006**, *244*, 349–360. [[CrossRef](#)]
39. Cocks, L.R.M.; Torsvik, T.H. Baltica from the late Precambrian to mid-Palaeozoic times: The gain and loss of a terrane's identity. *Earth-Sci. Rev.* **2005**, *72*, 39–66. [[CrossRef](#)]
40. Dzik, J. Ordovician conodonts and the Tornquist Lineament. *Palaeogeogr. Palaeoclim. Palaeoecol.* **2020**, *549*, 109157. [[CrossRef](#)]
41. Trela, W. Litostratygrafia ordowiku w Górach Świętokrzyskich. *Przegląd Geol.* **2006**, *54*, 622–631.
42. Trela, W. Eustatic and local tectonic impact on the Late Ordovician—Early Silurian facies evolution on the SW margin of peri-Baltica (the southern Holy Cross Mountains, Poland). *Geol. Mag.* **2021**, *158*, 1472–1486. [[CrossRef](#)]
43. Trela, W. Upper Ordovician mudrock facies and trace fossils in the northern Holy Cross Mountains, Poland, and their relation to oxygen- and sea-level dynamics. *Palaeogeogr. Palaeoclim. Palaeoecol.* **2007**, *246*, 488–501. [[CrossRef](#)]
44. Dzik, J. Conodonts of the Mójcza Limestone. *Paleontol. Pol.* **1994**, *53*, 43–128.
45. Dzik, J. Evolution of the Late Ordovician high-latitude conodonts and dating of Gondwana glaciations. *Boll. Della Soc. Paleontol. Ital.* **1998**, *37*, 237–253.
46. Dzik, J.; Pisera, A. Sedimentation and fossils of the Mójcza Limestones. *Paleontol. Pol.* **1994**, *53*, 5–41.
47. Trela, W. Condensation and phosphatization of the Middle and Upper Ordovician limestones on the Malopolska Block (Poland): Response to paleoceanographic conditions. *Sediment. Geol.* **2005**, *178*, 219–236. [[CrossRef](#)]
48. Tomczykowa, E.; Tomczyk, H. Rozwój badań syluru i najniższego dewonu w Górach Świętokrzyskich. *Przew* **1981**, *53*, 42–57.
49. Trela, W. Sedimentary and microbial record of the Middle/Late Ordovician phosphogenetic episode in the northern Holy Cross Mountains, Poland. *Sediment. Geol.* **2008**, *203*, 131–142. [[CrossRef](#)]

50. Lécuyer, C.; Amiot, R.; Touzeau, A.; Trotter, J. Calibration of the phosphate $\delta^{18}\text{O}$ thermometer with carbonate–water oxygen isotope fractionation equations. *Chem. Geol.* **2013**, *347*, 217–226. [[CrossRef](#)]
51. Belka, Z. Thermal maturation and burial history from conodont colour alteration data, Holy Cross Mountains, Poland. *Cour. Forsch.-Inst. Senckenberg* **1990**, *118*, 241–251.
52. Szczepanik, Z.; Malec, J. *Reżim Termiczny Obszaru Świętokrzysko-Nidziańskiego Oraz Pozycja Paleogeograficzna Gór Świętokrzyskich w Świetle Badań Paleozoicznych Flory i Fauny*; No. 2331/2001. (Archival study); National Geological Archives-Polish Geological Institute: Warsaw, Poland, 2001.
53. Trotter, J.; Williams, I.; Nicora, A.; Mazza, M.; Rigo, M. Long-term cycles of Triassic climate change: A new $\delta^{18}\text{O}$ record from conodont apatite. *Earth Planet. Sci. Lett.* **2015**, *415*, 165–174. [[CrossRef](#)]
54. Rigo, M.; Trotter, J.A.; Preto, N.; Williams, I.S. Oxygen isotopic evidence for Late Triassic monsoonal upwelling in the northwestern Tethys. *Geology* **2012**, *40*, 515–518. [[CrossRef](#)]
55. Narkiewicz, M.; Narkiewicz, K.; Krzemińska, E.; Kruchek, S.A. Oxygen isotopic composition of conodont apatite in the equatorial epeiric Belarussian Basin (Eifelian)—Relationship to fluctuating seawater salinity and temperature. *Palaios* **2017**, *32*, 439–447. [[CrossRef](#)]
56. Cooper, R.; Sadler, P.; Hammer, O.; Gradstein, F. The Ordovician Period. In *The Geologic Time Scale*; Elsevier: Amsterdam, The Netherlands, 2012; pp. 489–523.
57. Trotter, J.; Williams, I.S.; Barnes, C.R.; Männik, P.; Simpson, A. New conodont $\delta^{18}\text{O}$ records of Silurian climate change: Implications for environmental and biological events. *Palaeogeogr. Palaeoclim. Palaeoecol.* **2016**, *443*, 34–48. [[CrossRef](#)]
58. Wheeley, J.R.; Smith, M.P.; Boomer, I. Oxygen isotope variability in conodonts: Implications for reconstructing Palaeozoic palaeoclimates and palaeoceanography. *J. Geol. Soc.* **2012**, *169*, 239–250. [[CrossRef](#)]
59. Wheeley, J.; Jardine, P.E.; Raine, R.; Boomer, I.; Smith, M.P. Paleocologic and paleoceanographic interpretation of $\delta^{18}\text{O}$ variability in Lower Ordovician conodont species. *Geology* **2018**, *46*, 467–470. [[CrossRef](#)]
60. Kolodny, Y.; Luz, B.; Navon, O. Oxygen isotope variations in phosphate of biogenic apatites, I. Fish bone apatite—Rechecking the rules of the game. *Earth Planet. Sci. Lett.* **1983**, *64*, 398–404. [[CrossRef](#)]
61. Joachimski, M.M.; van Geldern, R.; Breisig, S.; Buggisch, W.; Day, J. Oxygen isotope evolution of biogenic calcite and apatite during the Middle and Late Devonian. *Geol. Rundsch.* **2004**, *93*, 542–553. [[CrossRef](#)]
62. Veizer, J.; Ala, D.; Azmy, K.; Bruckschen, P.; Buhl, D.; Bruhn, F.; Carden, G.A.; Diener, A.; Ebner, S.; Godderis, Y.; et al. $^{87}\text{Sr}/^{86}\text{Sr}$, $\delta^{13}\text{C}$ and $\delta^{18}\text{O}$ evolution of Phanerozoic seawater. *Chem. Geol.* **1999**, *161*, 59–88. [[CrossRef](#)]
63. Veizer, J.; Godderis, Y.; François, L. Evidence for decoupling of atmospheric CO_2 and global climate during the Phanerozoic eon. *Nature* **2000**, *408*, 698–701. [[CrossRef](#)]
64. Jaffrés, J.B.; Shields, G.; Wallmann, K. The oxygen isotope evolution of seawater: A critical review of a long-standing controversy and an improved geological water cycle model for the past 3.4 billion years. *Earth-Sci. Rev.* **2007**, *83*, 83–122. [[CrossRef](#)]
65. Veizer, J.; Prokoph, A. Temperatures and oxygen isotopic composition of Phanerozoic oceans. *Earth-Sci. Rev.* **2015**, *146*, 92–104. [[CrossRef](#)]
66. Galili, N.; Shemesh, A.; Yam, R.; Brailovsky, I.; Sela-Adler, M.; Schuster, E.M.; Collom, C.; Bekker, A.; Planavsky, N.; Macdonald, F.A.; et al. The geologic history of seawater oxygen isotopes from marine iron oxides. *Science* **2019**, *365*, 469–473. [[CrossRef](#)]
67. Pucéat, E.; Joachimski, M.; Bouilloux, A.; Monna, F.; Bonin, A.; Motreuil, S.; Morinière, P.; Hénard, S.; Mourin, J.; Dera, G. Revised phosphate–water fractionation equation reassessing paleotemperatures derived from biogenic apatite. *Earth Planet. Sci. Lett.* **2010**, *298*, 135–142. [[CrossRef](#)]
68. Longinelli, A. Comment on work by Pucéat et al. (2010) on a revised phosphate–water fractionation equation. *Earth Planet. Sci. Lett.* **2013**, *377–378*, 378–379. [[CrossRef](#)]
69. Pucéat, E.; Joachimski, M.; Bouilloux, A.; Monna, F.; Bonin, A.; Motreuil, S.; Morinière, P.; Hénard, S.; Mourin, J.; Dera, G.; et al. Reply on Comment by Longinelli (2013) on a revised phosphate–water fractionation equation. *Earth Planet. Sci. Lett.* **2013**, *377–378*, 380–382. [[CrossRef](#)]
70. Halas, S.; Skrzypek, G.; Meier-Augenstein, W.; Pelc, A.; Kemp, H.F. Inter-laboratory calibration of new silver orthophosphate comparison materials for the stable oxygen isotope analysis of phosphates. *Rapid Commun. Mass Spectrom.* **2011**, *25*, 579–584. [[CrossRef](#)] [[PubMed](#)]
71. Pohl, A.; Donnadiou, Y.; Le Hir, G.; Buoncristiani, J.-F.; Vennin, E. Effect of the Ordovician paleogeography on the (in)stability of the climate. *Clim. Past* **2014**, *10*, 2053–2066. [[CrossRef](#)]
72. Jin, J.; Zhan, R.; Wu, R. Equatorial cold-water tongue in the Late Ordovician. *Geology* **2018**, *46*, 759–762. [[CrossRef](#)]
73. Sweet, W.C. *The Conodonts: Morphology, Taxonomy, Paleocology, and Evolutionary History of a Long-Extinct Animal Phylum*; Clarendon Press: New York, NY, USA, 1988.
74. Rasmussen, J.A.; Stouge, S. Baltoscandian conodont biofacies fluctuations and their link to Middle Ordovician (Darriwilian) global cooling. *Palaeontology* **2018**, *61*, 391–416. [[CrossRef](#)]
75. Zhang, T.; Trela, W.; Jiang, S.-Y.; Nielsen, J.K.; Shen, Y. Major oceanic redox condition change correlated with the rebound of marine animal diversity during the Late Ordovician. *Geology* **2011**, *39*, 675–678. [[CrossRef](#)]
76. Kolata, D.R.; Huff, W.D.; Bergström, S.M. *Ordovician K-Bentonites of Eastern North America*; Geological Society of America: Boulder, CO, USA, 1996.

77. Huff, W.D. Ordovician K-bentonites: Issues in interpreting and correlating ancient tephras. *Quat. Int.* **2008**, *178*, 276–287. [[CrossRef](#)]
78. Kiipli, T.; Dahlqvist, P.; Kallaste, T.; Kiipli, E.; Nõlvak, J. Upper Katian (Ordovician) bentonites in the East Baltic, Scandinavia and Scotland: Geochemical correlation and volcanic source interpretation. *Geol. Mag.* **2015**, *152*, 589–602. [[CrossRef](#)]
79. Trela, W.; Bąk, E.; Pańczyk, M. Upper Ordovician and Silurian ash beds in the Holy Cross Mountains, Poland: Preservation in mudrock facies and relation to atmospheric circulation in the Southern Hemisphere. *J. Geol. Soc.* **2017**, *175*, 352–360. [[CrossRef](#)]
80. Smolarek-Lach, J.; Marynowski, L.; Trela, W.; Wignall, P.B. Mercury Spikes Indicate a Volcanic Trigger for the Late Ordovician Mass Extinction Event: An Example from a Deep Shelf of the Peri-Baltic Region. *Sci. Rep.* **2019**, *9*, 3139. [[CrossRef](#)] [[PubMed](#)]
81. Dzik, J. Zespół konodontów jako wskaźnik zmian klimatu podczas epoki lodowej. *Przegląd Geol.* **1999**, *47*, 349–353.
82. Loi, A.; Ghienne, J.-F.; Dabard, M.; Paris, F.; Botquelen, A.; Christ, N.; Elaouad-Debbaj, Z.; Gorini, A.; Vidal, M.; Videt, B.; et al. The Late Ordovician glacio-eustatic record from a high-latitude storm-dominated shelf succession: The Bou Ingarf section (Anti-Atlas, Southern Morocco). *Palaeogeogr. Palaeoclim. Palaeoecol.* **2010**, *296*, 332–358. [[CrossRef](#)]